

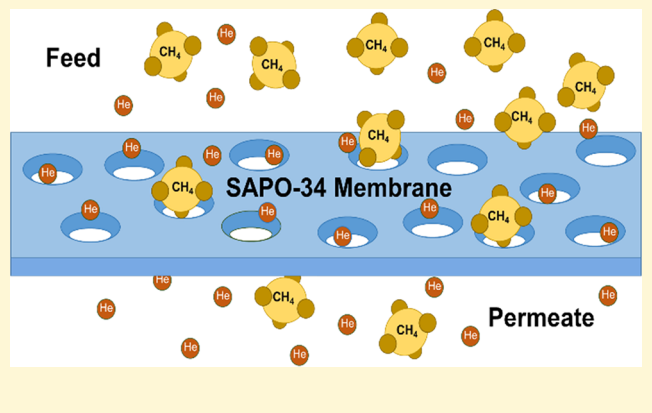
# Chabazite Zeolite SAPO-34 Membranes for He/CH<sub>4</sub> Separation

Shuraya Denning, Jolie Lucero, Carolyn A. Koh,<sup>id</sup> and Moises A. Carreon\*<sup>id</sup>

Chemical and Biological Engineering Department, Colorado School of Mines, Golden, Colorado 80401, United States

## Supporting Information

**ABSTRACT:** Natural gas reservoirs are the most abundant source of helium, despite helium being present only in trace amounts. Membrane technology represents an appealing and potentially cost-effective approach to recover helium from natural gas, consisting mainly of methane. Herein, we demonstrate that chabazite zeolite SAPO-34 membranes can effectively separate equimolar helium/methane mixtures. SAPO-34 membranes displayed helium permeance as high as  $2.28 \times 10^{-7}$  mol/(m<sup>2</sup> s Pa) and separation selectivity as high as 13.8 for He/CH<sub>4</sub> mixtures. The separation of this binary mixture was favored through molecular sieving and diffusivity differences. The best SAPO-34 membrane surpassed the Robeson limit upper bound, making these membranes appealing for helium recovery from natural gas.



Helium is a trace impurity found in natural gas and a highly desired product in the medical, scientific, and industrial markets as an inert gas and a cryogenic fluid.<sup>1,2</sup> Despite the abundance of helium on Earth,<sup>3</sup> the trace amount in natural gas is the primary commercial source of helium.<sup>2</sup> Industry commonly uses cryogenic distillation to separate out helium, a process which is energy-intensive, prone to equipment blockages, and expensive.<sup>4,5</sup> Membranes provide a potential alternative, because of multiple advantages,<sup>6,7</sup> such as no phase change, low environmental impact, and no moving parts (easy to use in remote locations).<sup>2</sup> A comprehensive review on membranes for helium recovery has been documented elsewhere.<sup>2</sup> In particular, zeolite membranes are highly appealing for diverse molecular gas separations, because of their hydrothermal, thermal, and chemical stability, permitting better performance under harsh operation conditions and for diverse gas mixtures.<sup>2</sup> The chabazite silico-aluminophosphate zeolite SAPO-34<sup>8,9</sup> has been demonstrated to effectively separate diverse industrially relevant gas mixtures, including CO<sub>2</sub>/CH<sub>4</sub>,<sup>10,11</sup> N<sub>2</sub>/CH<sub>4</sub>,<sup>12–14</sup> CO<sub>2</sub>/N<sub>2</sub>,<sup>15,16</sup> CO<sub>2</sub>/i-butane,<sup>17</sup> CO<sub>2</sub>/H<sub>2</sub>,<sup>18,19</sup> H<sub>2</sub>/CH<sub>4</sub>,<sup>18</sup> H<sub>2</sub>/N<sub>2</sub>,<sup>19</sup> air/Xe,<sup>20</sup> and Kr/Xe,<sup>21,22</sup> among others. The well-known molecular sieving ability of SAPO-34 prompted us to evaluate the separation performance of this zeolite for helium/methane mixtures, as the pore size of SAPO-34 is 3.8 Å<sup>23</sup> and the kinetic diameter of helium and methane is 2.6 and 3.8 Å, respectively.<sup>24</sup> Furthermore, SAPO-34 membranes are considered as potentially suitable candidates for large-scale application.<sup>25</sup> Herein, we demonstrate the ability of SAPO-34 membranes to separate equimolar mixtures of He/CH<sub>4</sub>.

SAPO-34 membranes were synthesized via secondary seeded growth, as described in the [Supporting Information](#). Figure 1

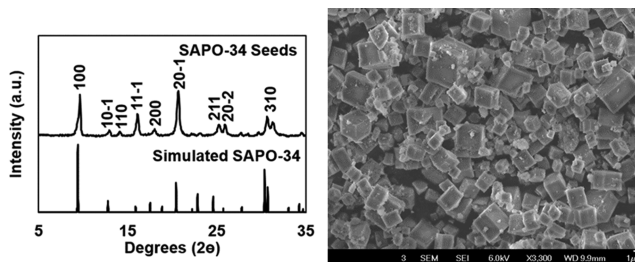


Figure 1. (a) Powder X-ray diffraction (PXRD) pattern and (b) representative scanning electron microscopy (SEM) image of the SAPO-34 crystals employed as seeds for membrane synthesis.

shows the powder X-ray diffraction (PXRD) pattern and a representative scanning electron microscopy (SEM) image of the SAPO-34 crystals employed as seeds for membrane synthesis. The XRD pattern of the seeds (see Figure 1a) agrees well with the chabazite topology that is characteristic of SAPO-34. Figure 1b shows the cubic structure of the SAPO-34 seeds, with an average crystal size of  $1.9 \pm 0.2 \mu\text{m}$ . Previous work on the role of seeds in synthesizing SAPO-34 membranes found that crystal size greatly affected membrane CO<sub>2</sub>

Received: August 13, 2019

Accepted: November 6, 2019

Published: November 6, 2019

separation performance, because of the narrow distribution size of the seeds.<sup>26</sup> Specifically, it was found that smaller SAPO-34 seed crystals with a narrow size distribution resulted in significantly higher selectivity and  $\text{CO}_2$  permeance, indicating that the smaller seeds can produce thinner membranes with more closely packed and smaller intergrown crystals.<sup>26</sup>

Five membranes were prepared with two water molar ratios: 150 and 300 (see the *Supporting Information* for experimental details). As shown in Figure S2 in the Supporting Information, the PXRD patterns of the crystals collected from the gel of the membranes confirmed the formation of chabazite topology. The molar ratios selected were used based on our previous report, which concluded that the extent of dilution of the synthesis gel correlated with a change in membrane thickness and crystal size.<sup>21</sup> The molar ratio of 150 produced a thicker membrane than the molar ratio of 300, providing a comparison to determine how the thickness of the membrane affects the separation performance. As shown in Figure 2, the SEM top and side views of the membrane show the same correlation

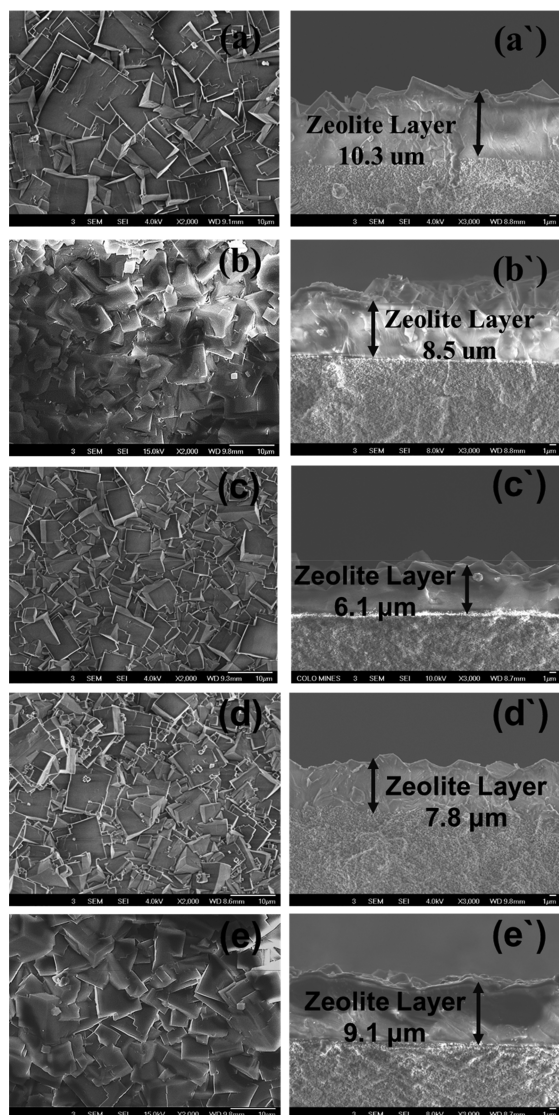


**Figure 2.** SEM images for the top view (left) and the cross-sectional view (right) of SAPO-34 membranes. Images (a, a'), (b, b'), (c, c'), (d, d'), and (e, e') represent M1, M2, M3, M4, and M5, respectively.

between dilution and membrane thickness/crystal size. The membranes with concentrated synthesis gel with a water molar ratio of 150 resulted in the thickest membranes and contained the largest crystals shown in images (a, a') and (b, b'). The diluted synthesis gel with a water molar ratio of 300 resulted in thinner membranes with smaller crystal sizes, illustrated in images (c, c'), (d, d'), and (e, e'). The thinner membrane is desired because it allows enhanced diffusion of the gas molecules, while the smaller crystal size typically leads to a better packing and, thus, a more even (regular) membrane thickness. The membranes with the lowest molar ratio of 150 (M1 and M2) were  $10.3 \pm 1.0$  and  $9.4 \pm 1.0 \mu\text{m}$  thick, respectively. For the membranes with the higher ratio of 300 (M3, M4, and M5), their respective thicknesses were  $6.1 \pm 0.3 \mu\text{m}$ ,  $7.0 \pm 0.8 \mu\text{m}$ , and  $9.1 \pm 0.4 \mu\text{m}$ . The top view of the crystals shows an average crystal size of  $14.4 \pm 8.5 \mu\text{m}$  for M1 and M2, and  $10.4 \pm 7.2 \mu\text{m}$  for M3, M4, and M5.

The synthesized SAPO-34 membranes were evaluated for the separation of an equimolar premixed  $\text{He}/\text{CH}_4$  mixture. Table 1 summarizes the separation data for these tests. To assess membrane reproducibility, two membranes were prepared independently with a water ratio of 150, and three membranes were prepared with a water molar ratio of 300.

The helium permeance ranged from  $1.37 \times 10^{-7} \text{ mol}/(\text{m}^2 \text{ s Pa})$  to  $2.28 \times 10^{-7} \text{ mol}/(\text{m}^2 \text{ s Pa})$ , and the separation selectivity ranged from 2.8 to 13.8. Generally, the thinner membranes led to higher helium permeance on average and a higher separation selectivity, as shown in Table 1. The high helium permeance and moderate separation selectivity observed resulted (in part) because of the intrinsic molecular sieving property of SAPO-34. In principle, the small size of the helium molecule ( $\sim 2.6 \text{ \AA}$ ) favors its diffusion through the  $3.8 \text{ \AA}$  pores of SAPO-34, while methane with a kinetic diameter of  $3.8 \text{ \AA}$  at best diffuses slowly through the chabazite framework.<sup>24</sup> As shown in a previous study by Carreon et al., the smaller crystal size correlates with better separation performance.<sup>26</sup> When comparing crystal sizes (Figure 2, left column), the larger crystal size can tend to create gaps between the crystals, increasing the chance of defects occurring in the membrane. The crystal size may explain why the selectivities of M1 and M2 are significantly lower than those of M3, M4, and M5. Defects decrease the number of selective pore pathways, which can cause a decrease in the desirable molecular sieving, because of the nonselective pores being larger than the kinetic diameter of  $\text{CH}_4$ . The  $\text{CH}_4$  can compete diffusively with  $\text{He}$  and, therefore, the increase in  $\text{CH}_4$  permeance causes a decrease in separation selectivity. Permeabilities will be strongly dependent on several factors, including membrane thickness, concentration of defects, and crystal intergrowth, among others. The contribution of defects on helium permeances cannot be ruled out.

The separation index ( $\pi$ ) provides a performance parameter to evaluate the reproducibility of membranes:<sup>11</sup>

$$\pi = \text{He permeance} \times (\text{selectivity} - 1) \times \text{permeate pressure}$$

For M1 and M2, prepared with a water content of 150, the separation indexes were  $3.1 \times 10^{-2}$  and  $2.4 \times 10^{-2}$ , respectively. The relatively small difference between these indexes indicate that, for this water molar ratio, the membranes show high reproducibility. For membranes M3, M4, and M5, the separation indexes range from  $9.5 \times 10^{-2}$  to  $21 \times 10^{-2}$ . The variation in separation indexes for this group of membranes may be related (at least in part) to several factors,

**Table 1. Separation Performance of SAPO-34 Membranes for a 50:50 He/CH<sub>4</sub> Mixture<sup>a</sup>**

water molar ratio	membrane ID	membrane thickness (μm)	He permeance (× 10 <sup>-7</sup> mol/m <sup>2</sup> s Pa)	separation selectivity, $\alpha$	separation index, $\pi$ (× 10 <sup>-2</sup> mol/m <sup>2</sup> s)
150	M1	10.3	1.52	3.4	3.1
150	M2	9.4	1.54	2.8	2.4
300	M3	6.1	2.28	8.2	13.7
300	M4	7.8	1.88	13.8	21.0
300	M5	9.1	1.37	9.2	9.5

<sup>a</sup>Transmembrane pressure = 138 kPa, flow rate = 30 sccm, room temperature.

including membrane thickness differences, concentration of defects, and plane preferential exposure. In this respect, the most selective membrane (M4) displayed preferential exposure of the most prominent XRD peak at  $2\theta \approx 9.4^\circ$ , corresponding to the (100) plane of chabazite (see Figure S2 in the Supporting Information). Interestingly, the intensity ratio of the most prominent peak of SAPO-34 corresponding to plane (100) to the secondary plane (101̄), denoted as  $I_{100}/I_{101̄}$ , correlated with the separation selectivity of the membranes, as shown in Figure S3 in the Supporting Information. Specifically, the higher  $I_{100}/I_{101̄}$  ratio led to the most selective membrane, while the lowest  $I_{100}/I_{101̄}$  ratio to the least selective membrane. The preferential exposure of a particular crystallographic plane in porous crystals can be associated with the presence of a high concentration of small crystallites.<sup>27</sup>

The differences in the rate of diffusion for He and CH<sub>4</sub> significantly affected the separation performance, since methane (16.04 g/mol) is considerably heavier than helium (4.00 g/mol), resulting in helium diffusing through the membrane faster, as compared to methane. To further understand and quantify this difference, the effective diffusion coefficients for each membrane were calculated. The coefficients were calculated using Fick's Law, which takes into account the gas flux through the membrane, the difference in concentration across the membrane, and the membrane thickness. Note that since these coefficients were obtained from membrane experiments, they implicitly include adsorption effects. These results, which are shown in Table 2 suggest

the degree of adsorption.<sup>23</sup> The relatively higher polarity of methane, compared to helium, results in methane preferential adsorption, as the zeolite's hydrophilic nature promotes adsorption of small polar molecules.<sup>24</sup> Methane has a polarizability of 2.448 Å<sup>3</sup>, which is relatively high, as compared to the polarizability of helium (0.208 Å<sup>3</sup>).<sup>24</sup> The framework of SAPO-34 is an anionic framework, giving the surface a net negative charge and, thus, interacting strongly with the most polarizable molecule and promoting its adsorption.<sup>23,28</sup> The polarizability couples with the higher condensability and larger molecular size of methane, compared to helium, resulting in a significantly higher adsorption coefficient for methane than helium.<sup>20</sup> The preferential adsorption of methane over helium competes with the diffusion and molecular sieving, causing the separation selectivity to be moderate.

The stability of membrane M4, which is the highest performing membrane in this study, was tested over a period of 5 days. The He permeance and He/CH<sub>4</sub> selectivity increased after 5 days by ~23% and 12%, respectively. These results indicate that SAPO-34 membranes display good long-term stability.

When comparing our separation data with previous reports on SAPO-34 membranes for other gas mixtures including H<sub>2</sub>/CH<sub>4</sub><sup>18</sup> and CO<sub>2</sub>/N<sub>2</sub><sup>19</sup> the following conclusions can be drawn. For H<sub>2</sub>/CH<sub>4</sub> separation over SAPO-34 membranes, the authors found that CH<sub>4</sub> adsorption inhibited H<sub>2</sub>, resulting in competitive adsorption; yet, this effect was outweighed by H<sub>2</sub> diffusing faster than CH<sub>4</sub> and the molecular sieving, because of the difference in kinetic diameters.<sup>18</sup> Despite the similar separation mechanisms, the separation selectivity of H<sub>2</sub> from CH<sub>4</sub> was higher (~20) than what we observed for He/CH<sub>4</sub> mixtures. This is likely due to the difference in the polarizability of He (0.208 Å<sup>3</sup>) versus the polarizability of H<sub>2</sub> (0.787 Å<sup>3</sup>). Hydrogen adsorbs preferentially (as compared to helium) over SAPO-34, because of its higher polarizability resulting in higher separation selectivities. Conversely, the permeance of He in our study is greater than that reported for H<sub>2</sub>/CH<sub>4</sub> mixtures.<sup>18</sup> The kinetic diameters of He and H<sub>2</sub> are 2.60 and 2.89 Å, respectively; therefore, in principle, the smaller He atom would diffuse faster than hydrogen within the SAPO-34 framework. When comparing the separation data for H<sub>2</sub>/CO<sub>2</sub> mixtures,<sup>19</sup> similar conclusions can be made. Specifically, the hydrogen diffusion rate of H<sub>2</sub> dominates over the competitive adsorption of CO<sub>2</sub>.

We compared the separation performance of SAPO-34 membranes to the state of the art membranes, using a Robeson plot revised and updated by Soleimany et al.<sup>29,7</sup> Figure 3 illustrates this comparison. The SAPO-34 membranes with high molar ratios (M3, M4, and M5) surpassed the 2008 Robeson upper limit of separation while the low molar ratio membranes (M1 and M2) lie between the prior and present

**Table 2. Effective Diffusion Coefficients for 50:50 He/CH<sub>4</sub> Mixture Permeated through SAPO-34 Membranes at Room Temperature with a Transmembrane Pressure of 138 kPa**

water molar ratio	membrane ID	$D(\text{He})$ (× 10 <sup>-10</sup> m <sup>2</sup> /s)	$D(\text{CH}_4)$ (× 10 <sup>-10</sup> m <sup>2</sup> /s)	$D(\text{He})/D(\text{CH}_4)$
150	M1	29.0	13.1	2.2
150	M2	28.4	14.3	2.0
300	M3	18.5	5.5	3.4
300	M4	13.5	3.2	4.2
300	M5	15.0	4.1	3.7

that helium diffuses ~2–4.2 times faster than CH<sub>4</sub> through SAPO-34 membranes. The lower performance of the thicker, lower water molar ratio membranes M1 and M2 correlates with a lower ratio of diffusion coefficient for He/CH<sub>4</sub>. The best performing membranes (M3–M5) display the highest He/CH<sub>4</sub> diffusivities.

Based on molecular sieving effects and higher He to CH<sub>4</sub> diffusivities, one may expect higher separation selectivity. However, the separation may be affected by the preferential adsorption of methane to the surface of SAPO-34. The stronger adsorption of methane over SAPO-34 is due to its polarity and polarizability, with the latter primarily determining

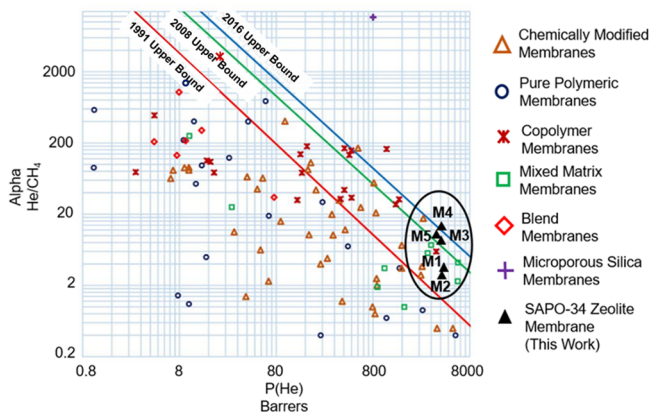


Figure 3. An updated 2008 Robeson plot by Soleimany et al., including results published as of 2016 for  $\text{He}/\text{CH}_4$  membrane separation performance.<sup>7,29</sup> The black triangles refer to the experimental results of this study.

Robeson upper bounds. Our best SAPO-34 membrane surpassed the updated Robeson upper bound limit.

The primary membranes for  $\text{He}/\text{CH}_4$  separation that approach the upper bound limit (such as Hyflon AD60X and Teflon AF-2400) or exceed it (such as poly(*p*-phenylene benzobisimidazole)) are polymeric membranes.<sup>7,28</sup> Despite the desirable separation performance, polymeric membranes may have some notable limitations, such as low thermal, chemical, and hydrothermal stability, leading to plasticization and swelling.<sup>2</sup> Silica membranes outperform polymers, in terms of thermal and chemical stability, yet are costly and time-consuming to synthesize.<sup>2</sup> Metal organic framework membranes and mixed-matrix membranes lack chemical, hydrothermal, and thermal stability, are costly to synthesize, and have flexible pore sizes, because of the organic component.<sup>2</sup> Zeolites provide high chemical, hydrothermal, and thermal stability.<sup>2</sup> The stability allows zeolites to potentially separate in the presence of multiple impurities under harsh conditions, thus saving costs, with regard to renewing or replacing the membrane. The ability of SAPO-34 membranes to effectively separate nitrogen, carbon dioxide, hydrogen, and helium (this work) from methane has been demonstrated. The overall separation performance of the SAPO-34 membranes in the presence of other impurities, will likely decrease, because of a strong competitive adsorption between the involved molecules.<sup>30,31</sup> This has been observed for SAPO-34 membranes employed for gas separations related to natural gas processing.

In conclusion, SAPO-34 membranes successfully separated helium from methane with the highest separation selectivity and helium permeance, reaching  $2.28 \times 10^{-7} \text{ mol}/(\text{m}^2 \text{ s Pa})$  and 13.8, respectively, at 273 K and a transmembrane pressure of 138 kPa. The best SAPO-34 membrane surpassed the revised Robeson upper bound limit, making these membranes good candidates for helium recovery from natural gas. Mechanistically, differences in diffusivities between the permeating molecules, and intrinsic molecular sieving of SAPO-34, led to helium selective membranes.

## ■ ASSOCIATED CONTENT

### Supporting Information

The Supporting Information is available free of charge on the ACS Publications website at DOI: [10.1021/acsmaterialslett.9b00324](https://doi.org/10.1021/acsmaterialslett.9b00324).

Experimental procedure for SAPO-34 seed and membrane synthesis; equipment description for membrane characterization and evaluation of gas separation performance; powder XRD pattern for crystals from each membrane (PDF)

## ■ AUTHOR INFORMATION

### Corresponding Author

\*E-mail: [mcarreon@mines.edu](mailto:mcarreon@mines.edu).

ORCID 

Carolyn A. Koh: [0000-0003-3452-4032](https://orcid.org/0000-0003-3452-4032)

Moises A. Carreon: [0000-0001-6391-2478](https://orcid.org/0000-0001-6391-2478)

### Notes

The authors declare no competing financial interest.

## ■ ACKNOWLEDGMENTS

M.A.C. and C.A.K. thank National Science Foundation (CBET Award No. 1835924) for financial support. S.D. thanks Ting Wu for useful advice on membrane synthesis.

## ■ REFERENCES

- Kidney, A.; Parrish, W.; McCartney, D. *Fundamentals of Natural Gas Processing*, 2nd Edition; CRC Press: Boca Raton, FL, 2011.
- Sunarso, J.; Hashim, S.; Lin, Y.; Liu, S. Membranes for helium recovery: An overview on the context, materials and future directions. *Sep. Purif. Technol.* **2017**, *176*, 335–383.
- King, H. Helium: A byproduct of the natural gas industry; available via the Internet at: <https://geology.com/articles/helium/> (accessed April 8, 2019).
- Rufford, T.; Chan, K.; Huang, S.; May, E. A review of conventional and emerging process technologies for the recovery of helium from natural gas. *Adsorpt. Sci. Technol.* **2014**, *32*, 49–72.
- Carreon, M. A. Molecular sieve membranes for  $\text{N}_2/\text{CH}_4$  separation. *J. Mater. Res.* **2018**, *33*, 32–43.
- Bernardo, P.; Drioli, E.; Golemme, G. Membrane gas separation: a review/state of the art. *Ind. Eng. Chem. Res.* **2009**, *48*, 4638–4663.
- Robeson, L. The upper bound revisited. *J. Membr. Sci.* **2008**, *320*, 390–400.
- Lixiong, Z.; Mengdong, J.; Enze, M. Synthesis of SAPO-34/ceramic composite membranes. *Stud. Surf. Sci. Catal.* **1997**, *105*, 2211–2216.
- Falconer, J.; Carreon, M. A.; Li, S.; Noble, R. Synthesis of zeolites and zeolite membranes using multiple structure directing agents, U.S. Patent No. 8,302,782, 2012.
- Li, S.; Falconer, J. L.; Noble, R. D. SAPO-34 membranes for  $\text{CO}_2/\text{CH}_4$  separations: Effect of Si/Al ratio. *Microporous Mesoporous Mater.* **2008**, *110*, 310–317.
- Carreon, M. A.; Li, S.; Falconer, J. L.; Noble, R. D. SAPO-34 Seeds and Membranes Prepared Using Multiple Structure Directing Agents. *Adv. Mater.* **2008**, *20*, 729–732.
- Li, S.; Zong, Z.; Zhou, S.; Huang, Y.; Song, Z.; Feng, X.; Zhou, R.; Meyer, H. S.; Yu, M.; Carreon, M. A. SAPO-34 Membranes for  $\text{N}_2/\text{CH}_4$  separation: Preparation, characterization, separation performance and economic evaluation. *J. Membr. Sci.* **2015**, *487*, 141–151.
- Zong, Z.; Feng, X.; Huang, Y.; Song, Z.; Zhou, R.; Zhou, S. J.; Carreon, M. A.; Yu, M.; Li, S. Highly permeable  $\text{N}_2/\text{CH}_4$  separation SAPO-34 membranes synthesized by diluted gels and increased crystallization temperature. *Microporous Mesoporous Mater.* **2016**, *224*, 36–42.
- Huang, Y.; Wang, L.; Song, Z.; Li, S.; Yu, M. Growth of High-Quality, Thickness-Reduced Zeolite Membranes towards  $\text{N}_2/\text{CH}_4$  Separation Using High-Aspect-Ratio Seeds. *Angew. Chem., Int. Ed.* **2015**, *54*, 10843–10847.
- Li, S.; Fan, C. Q. High-Flux SAPO-34 Membrane for  $\text{CO}_2/\text{N}_2$  Separation. *Ind. Eng. Chem. Res.* **2010**, *49*, 4399–4404.

(16) Venna, S. R.; Carreon, M. A. Amino-Functionalized SAPO-34 Membranes for CO<sub>2</sub>/CH<sub>4</sub> and CO<sub>2</sub>/N<sub>2</sub> Separation. *Langmuir* **2011**, *27*, 2888–2894.

(17) Wu, T.; Diaz, M.; Zheng, Y.; Zhou, R.; Funke, H.; Falconer, J.; Noble, R. Influence of propane on CO<sub>2</sub>/CH<sub>4</sub> and N<sub>2</sub>/CH<sub>4</sub> separations in CHA zeolite membranes. *J. Membr. Sci.* **2015**, *473*, 201–209.

(18) Hong, M.; Li, S.; Falconer, J. L.; Noble, R. D. Hydrogen purification using a SAPO-34 membrane. *J. Membr. Sci.* **2008**, *307*, 277–283.

(19) Das, J. K.; Das, N.; Bandyopadhyay, S. Highly oriented improved SAPO 34 membrane on low cost support for hydrogen gas separation. *J. Mater. Chem. A* **2013**, *1*, 4966–4973.

(20) Wu, T.; Lucero, J.; Crawford, J. M.; Sinnwell, M. A.; Thallapally, P. K.; Carreon, M. A. SAPO-34 membranes for xenon capture from air. *J. Membr. Sci.* **2019**, *573*, 288–292.

(21) Feng, X.; Zong, Z.; Elsaiedi, S. K.; Jasinski, J. B.; Krishna, R.; Thallapally, P. K.; Carreon, M. A. Kr/Xe Separation over a Chabazite Zeolite Membrane. *J. Am. Chem. Soc.* **2016**, *138*, 9791–9794.

(22) Kwon, Y. H.; Kiang, C.; Benjamin, E.; Crawford, P.; Nair, S.; Bhave, R. Krypton–xenon separation properties of SAPO-34 zeolite materials and membranes. *AIChE J.* **2017**, *63*, 761–769.

(23) Breck, D. W. *Zeolite Molecular Sieves: Structure, Chemistry, and Use*; John Wiley & Sons, Inc.: New York, 1974.

(24) Tagliabue, M.; Farrusseng, D.; Valencia, S.; Aguado, S.; Ravon, U.; Rizzo, C.; Corma, A.; Mirodatos, C. Natural gas treating by selective adsorption: Material science and chemical engineering interplay. *Chem. Eng. J.* **2009**, *155*, 553–566.

(25) Yu, M.; Noble, R. D.; Falconer, J. L. Zeolite Membranes: Microstructure Characterization and Permeation Mechanisms. *Acc. Chem. Res.* **2011**, *44*, 1196–1206.

(26) Carreon, M. A.; Li, S.; Falconer, J.; Noble, R. Alumina-supported SAPO-34 membranes for CO<sub>2</sub>/CH<sub>4</sub> separation. *J. Am. Chem. Soc.* **2008**, *130*, 5412–5413.

(27) Carreon, M. A.; Gulants, V. V. Macroporous vanadium phosphorus oxide phases displaying three-dimensional arrays of spherical voids. *Chem. Mater.* **2002**, *14*, 2670–2675.

(28) Wang, X.; Shan, M.; Liu, X.; Wang, M.; Doherty, C. M.; Osadchii, D.; Kapteijn, F. High-Performance Polybenzimidazole Membranes for Helium Extraction from Natural Gas. *ACS Appl. Mater. Interfaces* **2019**, *11*, 20098–20103.

(29) Soleimany, A.; Hosseini, S.; Gallucci, F. Recent progress in developments of membrane materials and modification techniques for high performance helium separation and recovery: A review. *Chem. Eng. Process.* **2017**, *122*, 296–318.

(30) Wu, T.; Diaz, M. C.; Zheng, Y.; Zhou, R.; Funke, H. H.; Falconer, J. L.; Noble, R. D. Influence of propane on CO<sub>2</sub>/CH<sub>4</sub> and N<sub>2</sub>/CH<sub>4</sub> separations in CHA zeolite membranes. *J. Membr. Sci.* **2015**, *473*, 201–209.

(31) Li, S.; Alvarado, G.; Noble, R. D.; Falconer, J. L. Effects of impurities on CO<sub>2</sub>/CH<sub>4</sub> separations through SAPO-34 membranes. *J. Membr. Sci.* **2005**, *251*, 59–66.